Localization of Metal-Induced Gap States at the Metal-Insulator Interface: Origin of Flux Noise in SQUIDs and Superconducting Qubits

SangKook Choi, Dung-Hai Lee, Steven G. Louie, and John Clarke*

Department of Physics, University of California, Berkeley, California 94720, USA

Materials Sciences Division, Lawrence Berkeley National Laboratory, Berkeley, California 94720, USA

(Received 21 July 2009; published 3 November 2009)

The origin of magnetic flux noise in superconducting quantum interference devices with a power spectrum scaling as $1/f$ (f is frequency) has been a puzzle for over 20 years. This noise limits the decoherence time of superconducting qubits. A consensus has emerged that the noise arises from fluctuating spins of localized electrons with an areal density of 5×10^{17} m^{-2}. We show that, in the presence of potential disorder at the metal-insulator interface, some of the metal-induced gap states become localized and produce local moments. A modest level of disorder yields the observed areal density.

DOI: 10.1103/PhysRevLett.103.197001 PACS numbers: 85.25.Dq, 03.67.Lx, 05.40.Ca, 73.20.Fz

Well below 1 K, low-transition temperature superconducting quantum interference devices [1] (SQUIDs) exhibit magnetic flux noise [2] with a temperature-independent spectral density scaling as $1/f^{\alpha}$, where f is frequency and $0.6 \leq \alpha \leq 1$. The noise magnitude, a few $\mu\Phi_0$ Hz$^{-1/2}$ at 1 Hz (Φ_0 is the flux quantum), scales slowly with the SQUID area, and does not depend significantly on the nature of the thin-film superconductor or the substrate on which it is deposited. The substrate is typically silicon or sapphire, which are insulators at low temperature (T) [2]. Flux noise of similar magnitude is observed in flux [3,4] and phase [5] qubits. Flux noise limits the decoherence time of superconducting, flux sensitive qubits making scale-up for quantum computing problematic. The near insensitivity of noise magnitude to device area [2,5,6] suggests the origin of the noise is local. Koch *et al.* [7] proposed a model in which electrons hop stochastically between traps with different preferential spin orientations. A broad distribution of time constants is necessary to produce a $1/f$ power spectrum [8,9]. They found that the major noise contribution arises from electrons above and below the superconducting loop of the SQUID or qubit [5,7], and that an areal density of about 5×10^{17} m^{-2} unpaired spins is required to account for the observed noise magnitude. De Sousa [10] proposed that the noise arises from spin flips of paramagnetic dangling bonds at the Si-SiO_2 interface. Assuming an array of localized electrons, Faoro and Ioffe [11] suggested that the noise results from electron spin diffusion. Sendelbach *et al.* [12] showed that thin-film SQUIDs are paramagnetic, with a Curie ($1/T$) susceptibility. Assuming the paramagnetic moments arise from localized electrons, they deduced an areal density of 5×10^{17} m^{-2}. Subsequently, Bluhm *et al.* [13] used a scanning SQUID microscope to measure the low-T paramagnetic response of (nonsuperconducting) Au rings deposited on Si substrates, and reported an areal density of 4×10^{17} m^{-2} for localized electrons. Paramagnetism was not observed on the bare Si substrate.

In this Letter we propose that the local magnetic moments originate in metal-induced gap states (MIGS) [14] localized by potential disorder at the metal-insulator interface. At an ideal interface, MIGS are states in the band gap that are evanescent in the insulator and extended in the metal [14] (Fig. 1). In reality, at a nonepitaxial metal-insulator interface there are inevitably random fluctuations in the electronic potential. The MIGS are particularly sensitive to these potential fluctuations, and a significant fraction of them—with single occupancy—becomes strongly localized near the interface, producing the observed paramagnetic spins. Fluctuations [15] of these local moments yield T-independent $1/f$ flux noise.

To illustrate the effects of potential fluctuations on the MIGS we start with a tight-binding model for the metal-insulator interface, consisting of the (100) face of a simple-cubic metal epitaxially joined to the (100) face of an insulator in a CsCl structure [Fig. 2(a)]. For the metal we assume a single s orbital per unit cell and nearest-neighbor (NN) hopping. For the insulator we place an s orbital on each of the two basis sites of the CsCl structure and assume both NN and next-nearest-neighbor (NNN) hopping. The parameters are chosen so that the metal s orbitals are at zero energy and connected by a NN hopping energy of -0.83 eV. The on-site energy of the orbitals on the Cs and

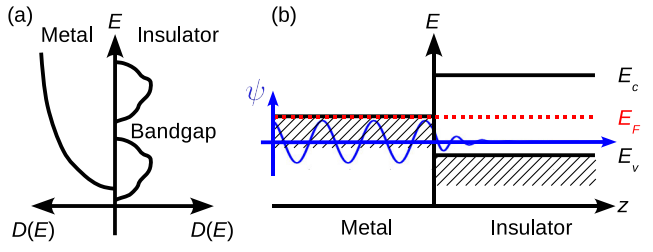

FIG. 1 (color online). (a) Schematic density of states. (b) MIGS at a perfect interface with energy in the band gap are extended in the metal and evanescent in the insulator.

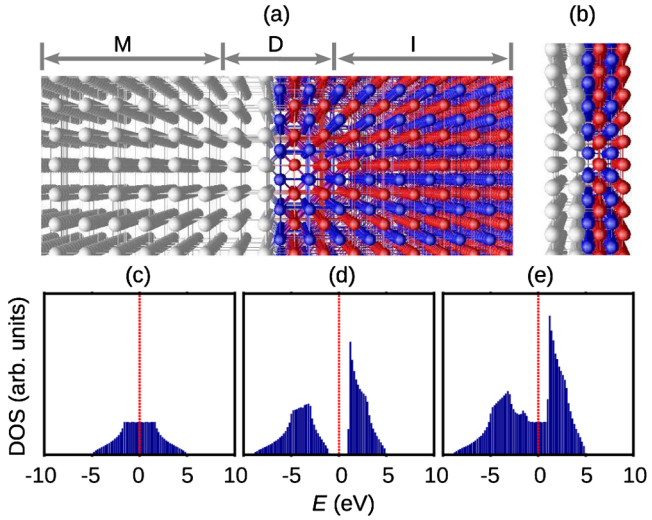

FIG. 2 (color online). (a) The metal (M) has a simple-cubic structure with one atom per unit cell and the insulator (I) a CsCl structure with two atoms per unit cell. (b) Interfacial region (D) consists of 2 layers of metal unit cells and 2 layers of insulator unit cells. The lattice constant is 0.15 nm. Computed DOS with Fermi energy (dotted red line) set to zero. (c) Typical metal with 10 eV bandwidth. (d) Typical insulator with a 2 eV band gap separating two bands of about 8 and 4 eV. (e) Metal-insulator interface with MIGS in the band gap of the insulator due to the presence of the metal.

Cl sites is taken to be -4 and 2 eV, respectively, and both the NN and NNN hopping energies are set to -0.5 eV. These parameters yield a band width of 10 eV for the metal, and 8 and 4 eV band widths, respectively, for the valence and conduction bands of the insulator with a band gap of 2 eV [Fig. 2(d)]. These band structure values are typical for conventional metals and for semiconductors and insulators. For the interface we take the hopping energy between the metallic and insulating atoms closest to the interface to be -0.67 eV, the arithmetic mean of -0.83 and -0.5 eV.

The electronic structure of the ideal metal-insulator junction is calculated using a supercell [16] containing $20 \times 20 \times 20$ metal unit cells and $20 \times 20 \times 20$ insulator unit cells, a total of 24 000 atoms. The total density of states (DOS) of the supercell [Fig. 2(e)] shows a nearly flat DOS in the band gap region. The states in the insulator band gap are MIGS that are extended in the metal, decaying rapidly away from the interface into the insulator. Our model with a lattice constant of 0.15 nm yields an areal density of states for the MIGS of about 3×10^{18} eV^{-1} m^{-2}, consistent with earlier self-consistent pseudopotential calculations [17].

To mimic the effects of interfacial randomness, we allow the on-site energy to fluctuate for both metal and insulator atoms near the interface [18]. Specifically we assume an energy distribution $P(E) = (1/\sqrt{2\pi}\delta) \times \exp[-(E - E_0)^2/2\delta^2]$, where E_0 is the original on-site energy without disorder, and δ is the standard deviation. We characterize the degree of disorder by the dimensionless ratio $R = 2\delta/W$, where W is the bandwidth of the metal. For those MIGS that become localized, the energy cost, U_i, for double occupation is large, and we cannot use a noninteracting electron approach. Instead we adopt a strategy similar to that used by Anderson in his calculation of local moment formation [19]. We separate the space near the interface into three regions: (i) the perfect metal region (M), (ii) an interfacial region consisting of 2 layers of metal unit cells and 2 layers of insulator unit cells (D) [Fig. 2(b)], and (iii) the perfect insulator region (I). Region (ii) is analogous to the impurity in Anderson's analysis.

We first compute the single-particle eigenstates, $\varphi_i(\mathbf{r})$, of region D in isolation. For each of these states, we compute U_i (using a long-range Coulomb potential with an on-site cutoff of 10 eV) and the hybridization energy Γ_i due to hopping to the metal and the insulator [20]. With the computed values of U_i and Γ_i, we solve Anderson's equation for the spin-dependent occupation for each localized state $|\, i\rangle$:

$$\langle n_{i,\sigma}\rangle = \frac{1}{\pi}\int_{-\infty}^{E_F} dE' \frac{\Gamma_i}{(E' - E_{i,\sigma})^2 + \Gamma_i^2}. \qquad (1)$$

Here, $E_{i,\sigma} = E_i + U_i\langle n_{i,-\sigma}\rangle$ and σ is the spin index. The net moment associated with the state is given by $m_i = \mu_B|\langle n_{i,\sigma}\rangle - \langle n_{i,-\sigma}\rangle|$. Equation (1) and the associated expression for the net moment of the localized states are calculated within the self-consistent Hartree-Fock approximation [19]. An $m_i \neq 0$ solution is obtained only when $U_i/(E_F - E_i)$ exceeds a critical value which depends on $\Gamma_i/(E_F - E_i)$. In the large U_i limit, it is more appropriate to start from the weak coupling limit ($\Gamma_i = 0$), where the localized state is populated by a single electron, and treat Γ_i as a perturbation. By calculating the areal density of such moment-bearing localized states we estimate the density of spin-$\frac{1}{2}$ local moments.

Figure 3 shows the calculated distribution $\rho(E, U)$ in the isolated interfacial region for $R = 0.05, 0.1, 0.15, 0.2, 0.25$, and 0.3; for each value, higher values of U correspond to more localized states. As expected we see that, for any given degree of randomness, the states with energy inside the insulator band gap (the MIGS) or those at the band edges are most susceptible to localization. Figure 4 shows a perspective plot of the charge density of two states, with high and low values of U_i, showing the correlation between the degree of wave function localization and the value of U_i. Both states are centered in the insulator, a general characteristic of localized states in the band gap originating from the MIGS.

Setting the Fermi energy at the insulator midgap value, we estimate the areal density of spins for a given degree of randomness R. The top panel in Fig. 5 depicts the distribution $\rho(E, m)$ of the spin moments as a function of energy. We see that for small R virtually all the local moments are

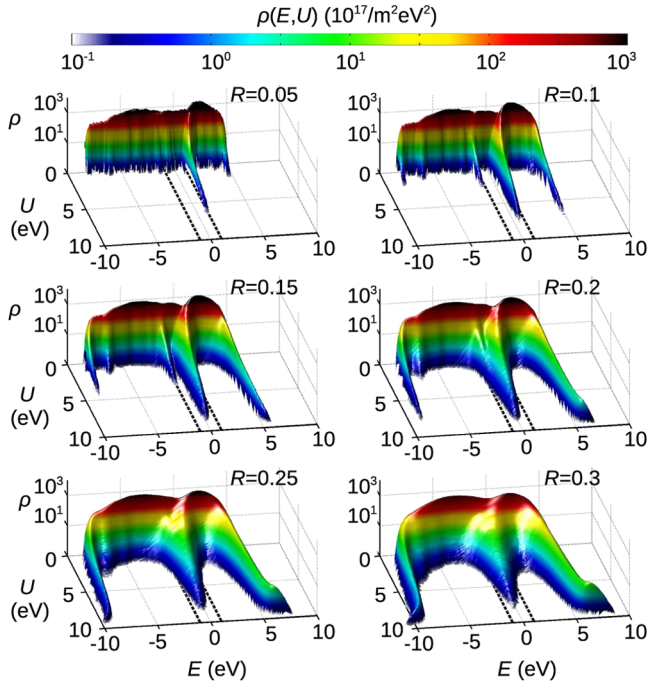

FIG. 3 (color online). Density of states distribution $\rho(E, U)$ as a function of energy E and Hubbard energy U for 6 values of the randomness parameter R in the isolated D region of Fig. 2. For a given value of R, the highest values of U, resulting in the most highly localized states, appear in the band gap of the insulator and at the band edges. The position of the insulator band gap is represented by black dashed lines.

derived from the MIGS. The bottom panel of Fig. 5 shows the calculated areal density of local moments versus R. Our simple model thus indicates that moderate potential fluctuations ($R \sim 0.15$) at the interface produce an areal density of localized moments comparable to experimental values [21]. Although our analysis is for a specific model, we expect the general physical picture to remain valid for

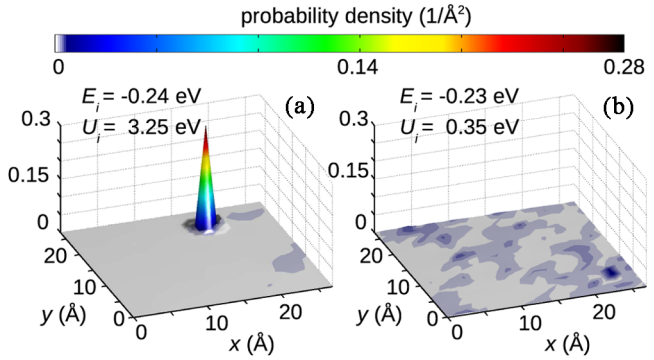

FIG. 4 (color online). Perspective view images of the two-dimensional probability density distribution at the interfacial region (D) along directions parallel to the interface (x and y directions), integrated along the z direction. (a) States with $U_i = 3.25$ eV and $E_i = -0.24$ eV and (b) with $U_i = 0.35$ eV and $E_i = -0.23$ eV, respectively.

real materials. First, the formation of MIGS at a metal-insulator interface is universal, and their areal density is rather insensitive to the nature of the materials as discussed in the supplementary material [20] and shown numerically in Ref. [17]. Second, the formation of local moments from the combination of localized states and Coulomb interaction is a general phenomenon [19]. We also note that our analysis should not be significantly modified when the metal is superconducting. This is because the U_i for the localized states is generally much greater than the pairing gap. Of course, extended states with negligible U_i would be paired.

Given our picture of the origin of the localized spin-$\frac{1}{2}$ moments, how do they produce $1/f$ flux noise with a spectral density $S_\Phi(f) \propto 1/f^\alpha$? The local moments interact via mechanisms such as direct superexchange and the RKKY interaction [11,23–25] between themselves, and Kondo exchange with the quasiparticles in the superconductor. This system can exhibit a spin-glass transition [26], which could account for the observed susceptibility cusp [12] near 55 mK. For $T > 55$ mK, however, experiments suggest that the spins are in thermal equilibrium [27] and exhibit a $1/T$ (Curie law) static susceptibility [12,13]. In this temperature regime, for $hf \ll k_B T$ standard linear

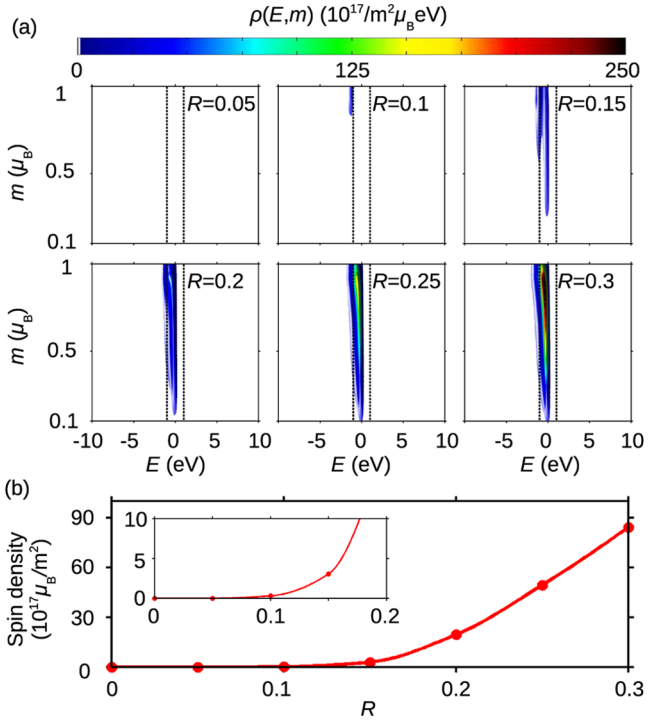

FIG. 5 (color online). (a) Electron density distribution $\rho(E, m)$ for 6 values of R. We simulated 5000 different configurations of disorder for each value of R. The position of the insulator band gap is represented by black dashed lines. Virtually all the magnetic moments are from the MIGS in the band gap of the insulator. (b) Integrated spin density versus randomness parameter R. For $R = 0.05$, we estimate the spin density to be less than 0.01×10^{17} m^{-2}.

response theory [28] shows that the imaginary part of the dynamical susceptibility $\chi''(f,T) = A(f,T)(hf/k_BT)$. Here, $A(f,T) \propto \sum_\mu \sum_{\alpha,\beta} P_\alpha \delta(hf + E_\alpha - E_\beta) |\langle \beta | S_\mu | \alpha \rangle|^2$, where S_μ is the μth component of the spin operator, α and β label the exact eigenstates, and P_α is the Boltzmann distribution associated with state α. Combining the above result with the fluctuation-dissipation theorem [15] which relates the flux noise to $\chi''(f,T)$, namely $S_\Phi(f,T) \propto (k_BT/hf)\chi''(f,T)$, we conclude that the observed $1/f^\alpha$ spectral density implies $A(f,T) \propto 1/f^\alpha (0.6 \leq \alpha \leq 1)$. Assuming low frequency contributions dominate the Kramers-Kronig transform, this result is consistent with the observed $1/T$ static susceptibility, and the recent measurement [29] showing that flux noise in a SQUID is highly correlated with fluctuations in its inductance, However, without knowing the form of the interaction between the spins, one cannot derive this behavior for $A(f,T)$ theoretically.

In conclusion, we have presented a theory for the origin of the localized magnetic moments which have been shown experimentally to give rise to the ubiquitous low-T flux $1/f$ noise observed in SQUIDs and superconducting qubits. In particular we have shown that for a *generic* metal-insulator interface, disorder localizes a substantial fraction of the metal-induced gap states (MIGS), causing them to bear local moments. Although MIGS have been known to exist at metal-insulator interfaces for three decades, we believe this is the first understanding of their nature in the presence of strong local correlation and disorder. Provided T is above any possible spin-glass transition, experiments show that fluctuations of these local moments produce a paramagnetic χ' and a power-law, f-dependent χ'' which in turn leads to flux $1/f$ noise. It is important to realize that localized MIGS occur not only at the metal-substrate interface but also at the interface between the metal and the oxide that inevitably forms on the surface of superconducting films such as aluminum and niobium. There are a number of open problems, for example, the precise interaction between the local moments, its relation to the value of α, and the possibility of a spin-glass phase at low temperature. A particularly intriguing experimental issue to address is why different metals and substrates evidently have such similar values of R, around 0.15. Experimentally, to improve the performance of SQUIDs and superconducting qubits we need to understand how to control and reduce the disorder at metal-insulator interfaces, for example, by growing the superconductor epitaxially on its substrate.

We thank R. McDermott and K. A. Moler for prepublication copies of their papers. S. C. and S. G. L. thank M. Jain and J. D. Sau for fruitful discussions. This work was supported by the Director, Office of Science, Office of Basic Energy Sciences, Materials Sciences and Engineering Division, of the U.S. Department of Energy under Contract No. DE-AC02-05CH11231. S. C. acknowledges support from the Samsung Foundation.

*jclarke@berkeley.edu

[1] J. Clarke and A. I. Braginski, *The SQUID Handbook* (Wiley-VCH, GmbH and Weinheim, 2004), Vol. 1.
[2] F. C. Wellstood, C. Urbina, and J. Clarke, Appl. Phys. Lett. **50**, 772 (1987).
[3] F. Yoshihara, K. Harrabi, A. O. Niskanen, Y. Nakamura, and J. S. Tsai, Phys. Rev. Lett. **97**, 167001 (2006).
[4] K. Kakuyanagi *et al.*, Phys. Rev. Lett. **98**, 047004 (2007).
[5] R. C. Bialczak *et al.*, Phys. Rev. Lett. **99**, 187006 (2007).
[6] T. Lanting *et al.*, Phys. Rev. B **79**, 060509(R) (2009).
[7] R. H. Koch, D. P. DiVincenzo, and J. Clarke, Phys. Rev. Lett. **98**, 267003 (2007).
[8] S. J. Machlup, J. Appl. Phys. **25**, 341 (1954).
[9] P. Dutta and P. M. Horn, Rev. Mod. Phys. **53**, 497 (1981).
[10] R. de Sousa, Phys. Rev. B **76**, 245306 (2007).
[11] L. Faoro and L. B. Ioffe, Phys. Rev. Lett. **100**, 227005 (2008).
[12] S. Sendelbach *et al.*, Phys. Rev. Lett. **100**, 227006 (2008).
[13] H. Bluhm, J. A. Bert, N. C. Koshnick, M. E. Huber, and K. A. Moler, Phys. Rev. Lett. **103**, 026805 (2009).
[14] S. G. Louie and M. L. Cohen, Phys. Rev. B **13**, 2461 (1976).
[15] H. Nyquist, Phys. Rev. **32**, 110 (1928).
[16] M. L. Cohen, M. Schlüter, J. R. Chelikowsky, and S. G. Louie, Phys. Rev. B **12**, 5575 (1975).
[17] S. G. Louie, J. R. Chelikowsky, and M. L. Cohen, Phys. Rev. B **15**, 2154 (1977).
[18] P. W. Anderson, Phys. Rev. **109**, 1492 (1958).
[19] P. W. Anderson, Phys. Rev. **124**, 41 (1961).
[20] See EPAPS Document No. E-PRLTAO-103-009946 for areal density of MIGS, Hubbard energy, and hybridization energy broadening. For more information on EPAPS, see http://www.aip.org/pubservs/epaps.html.
[21] If one includes the effect of metallic screening from region M on U_i (Ref. [22]), U_i would decrease by a factor of roughly 2 since the localized state in region I is located on average $\sim$3 unit cell layers from region M. We estimate this effect reduces the spin density by $\sim$50% at each R value. As a result, R should be increased by at most 10% to produce an areal density of $\sim 5 \times 10^{17}$ m^{-2}.
[22] J. D. Sau, J. B. Neaton, H. J. Choi, S. G. Louie, and M. L. Cohen, Phys. Rev. Lett. **101**, 026804 (2008).
[23] M. A. Ruderman and C. Kittel, Phys. Rev. **96**, 99 (1954).
[24] T. Kasuya, Prog. Theor. Phys. **16**, 45 (1956).
[25] K. Yosida, Phys. Rev. **106**, 893 (1957).
[26] M. B. Weissman, Rev. Mod. Phys. **65**, 829 (1993).
[27] R. Harris *et al.*, Phys. Rev. Lett. **101**, 117003 (2008).
[28] A. L. Fetter and J. D. Walecka, *Quantum Theory of Many-Particle Systems* (McGraw-Hill, New York, 1971), p. 298.
[29] S. Sendelbach, D. Hover, M. Mück, and R. McDermott, Phys. Rev. Lett. **103**, 117001 (2009).